ELSEVIER

Journal of Chromatography A, 872 (2000) 259–268

JOURNAL OF CHROMATOGRAPHY A

www.elsevier.com/locate/chroma

On-column amperometric detection in capillary electrophoresis with an improved high-voltage electric field decoupler

S.S. Zhang[a,b,*], Z.B. Yuan[b], H.X. Liu[a], H. Zou[b], Y.J. Wu[a]

[a]*Instrumental Analysis Center, Zhengzhou University, Zhengzhou 450052, China*

[b]*Department of Chemistry, Graduate School, University of Science and Technology of China, Chinese Academy of Sciences, Beijing 100039, China*

Received 14 July 1999; received in revised form 24 November 1999; accepted 26 November 1999

Abstract

An improved fabrication method for a decoupler for on-column amperometric detection in capillary electrophoresis (CE) is described. The decoupler is fabricated by etching one side-wall of the capillary with hydrofluoric acid after the polymer coating had been etched by laser, then the etched hole is sealed with adhesive. The steady time, electric conductivity efficiency and performance are investigated. On-column amperometric detection by CE of *para*-substituted phenols was carried out by coupling with a carbon-fiber microelectrode (10-μm diameter) and a practical small electrochemical detection cell.

Keywords: Instrumentation; Electrochemical detection; Detection, Electrophoresis; Phenols

1. Introduction

Since its introduction about a decade ago by Mikkers et al. [1] and Jorgenson et al. [2,3], capillary electrophoresis(CE) has been established as a powerful technique in the area of liquid phase separation. It has the advantages of extremely low mass detection limits, small sample volume, high speed, and high separation efficiency. A major limitation has been that the concentration detection limits are relatively high. Much considerable effort has been concentrated on the development of fluorescence [4–8] and electrochemical [9–14] detection (ED) for CE in order to lower the concentration detection limits. One of the major problems in CE–ED is that the interference of the high electric field used in the electrophoresis system gives rise to noise at the electrochemical detector. In general, the noise arising from the CE system has been the limiting factor in the detection limits of CE.

No significant interference from the high electric field in end-column amperometric detection is observed if narrow (2~25 μm) separation capillaries are applied for CE. But the narrow capillary causes the capillary to block and gives rise to the unstable position of the microelectrode at the end of the capillary.

With wider capillaries, off-column amperometric detection has to be used. The high-voltage electric field has to be decoupled before the detector, and the

*Corresponding author.

0021-9673/00/$ – see front matter
PII: S0021-9673(99)01260-1

solution with the separated zones will pass through the decoupler from separation capillary to detection capillary and finally arrives at the detector. Since the first porous glass joint [9] was used to decouple the high electric field, similar designs including the use of porous graphite tubing [15], Nafion tubing [10], cellulose acetate film [16], Pd tubing [17] and ionomer membrane [18,19] have been developed to solve the same problem. Hu et al. [12] constructed an etched joint by immersing the capillary in hydrofluoric acid to etch a part of the capillary wall. Huang and Zare [20] designed an on-column fit. This design is also difficult to implement as a laser-drilled hole in the capillary is required to construct the fit.

The joints described above possess the drawbacks of greater size, lower strength and reproducibility. In this paper, an improved method for fabricating the electric field decoupler without fracturing the capillary and the decoupler used in on-column amperometric detection in CE are described. The decoupler is fabricated by etching one side-wall of the capillary with hydrofluoric acid after the polymer coating had been etched by laser, then the etched hole is sealed with adhesive. In this way, a decoupler with a hole of diameter from 60 to 90 μm provides improved strength with lower dead volume, and can be easily fabricated.

The analysis of phenolic compounds is of importance to environmental regulatory agencies as these materials pose significant human and environmental hazards. There are some gas chromatography, liquid chromatography, capillary zone electrophoresis with amperometry [21] and micellar electrokinetic capillary chromatography methods with fluorescence detection [22] for the determination of phenolic compounds. These phenols are easily separated when the numbers of the substituted group are different. On the contrary, they are more difficult to separate when they hold the same numbers of substituted groups, especially when they hold the same position. In this report, using the improved high-voltage electric field decoupler and laboratory-made CE–ED system with small detection cell and carbon-fiber microelectrode [23], on-column amperometric detection of six *para*-substituted phenols (*p*-aminophenol, *p*-bromophenol, *p*-chlorophenol, *p*-diphenol, *p*-nitrophenol and *p-tert*.-butylphenol) has been carried out.

2. Experimental

2.1. Chemicals and solutions

All the chemicals were analytical-grade reagents from Beijing Chemical Factory (Beijing, China). Stock solutions of those phenols (*para*-substituted phenols), 100 mg/l, were prepared by dissolving 10±0.10 mg of each material into separate 100-ml volumetric flasks, which were filled with 10 m*M* Na_2HPO_4–NaH_2PO_4 (pH 6.5)–10 m*M* SDS.

Standard solutions were prepared by putting the stock solutions into 10-ml flasks. Then, the buffer was added to the vial for the standard solution concentrations of 50, 20, 10, 5.0, 3.0, 2.0, 1.0 and 0.5 mg/l, respectively.

The buffers and sample solutions injected into the capillary were filtered through a 0.4-μm membrane filter.

2.2. CE apparatus

A 1229 HPCE analyser (Beijing Institute of New Technology and Application, Beijing, China) with a fixed-wavelength UV detector at 280 nm was used in the comparison of the separation efficiency change (in theoretical plate number) by CE–ED with the improved high-voltage electric field decoupler. The d.c. high voltage was to be changed from 0 to 30 kV. Bare fused-silica capillaries were from Yongnian Optical Factory (Yongnian, Hebei Province, China). Capillary dimensions were 50 μm I.D.×375 μm O.D. The pHs of the buffers were measured using a No. 5994 pH meter (Cole-Parmer, Chicago, USA). Experiments were performed at ambient temperature (24°C) throughout. A fused-silica capillary was rinsed with 0.1 *M* NaOH and double-distilled water, respectively, and was then re-equilibrated with running buffer for 10 min.

2.3. Fabrication of the high-voltage electric field decoupler

The 27-nm laser from Quanta-Ray DCR-3 YAG Dye Pulse Laser (Spectra-Physics, USA) was focused at a location of 2–3 cm (detection capillary)

from the end of a 57-cm-long (or desired length) capillary. An approximately 20-μm etched spot in diameter was obtained by laser under the optimal laser energy at 35 J per pulse and frequency at 40 Hz for 2 s. The section with the etched spot was immersed in 40% hydrofluoric acid for etching. After the spot was etched for 7 h, a hole of 60~90 μm diameter appeared in the single side wall of the capillary. This hole was observed and sealed with ZD-61 glue (A+B, the main content is epoxy, made in our laboratory). After 1 h, the capillary was rinsed with water to prevent the capillary channel from being blocked up. Four h later, the coating was solidified at ambient temperature, meanwhile the decoupler was completed. Finally, the capillary with the completed decoupler was flushed in turn with EtOH, water, 0.1 *M* NaOH and water. The mechanical strength of the area where the etched spot contacts the ZD-61 glue was enhanced by casting the same glue around the etched spot. The coating thickness at about 0.3–0.4 mm was observed and calculated under a microscope. This decoupler has the advantages of high strength, small size and high-efficiency for isolating the electric field. It is durable; no apparent deterioration was observed after daily use over a six-month period. In addition, the decoupler was easily commercialized; we completed the fabrication with a 85% success rate.

2.4. Electrochemical detection

The electrochemical cell was made of an acrylic Plexiglass cylinder (diameter=4 mm, height=12 mm). Two separate holes with a diameter of 8 mm and height of 8 mm for laying the decoupler and reference electrode (Ag plate) were drilled while two smaller holes with 4-mm diameter by 8-mm height were among the larger holes. Both larger holes were called the decoupler hole (D-H) and detection hole (d-H), respectively. The channels (4-mm diameter) for cathode and reference electrode were connected with the D-H and d-H, respectively, drilled from the side wall of the Plexiglass. The separation capillary with a decoupler was placed across the D-H, both small holes and d-H while the decoupler was placed in D-H, and the end of the detection capillary was placed in the center of d-H. The electrochemical cell assembly was given in Ref. [23].

The carbon-fiber microelectrode was prepared by the following steps. First, a single carbon fiber (10-μm diameter, Goodfellow, London, UK) was fixed on the copper thread (0.4-mm diameter) with cellulose acetate adhesive (29.3% acetyl content), which was from Beijing Hongxing Chemical Factory and the carbon fiber protruded about 1 cm; secondly, the protruded carbon fiber was inserted through a common plastic pipette until the fiber protruded ~8 mm from the tip of the pipette, the other end of the Cu thread was fixed on the pipette by cycling; finally, the tip of the pipette was sealed with a little drop of cellulose acetate adhesive, the microelectrode was completed after the adhesive was dried at room temperature for 1 h. Carbon fibers exhibit interesting surface phenomena that can significantly influence the reversibility of redox reactions and the resulting voltammetric response. It has long been recognized that the pretreatment of carbon-fiber electrodes can have a dramatic effect on the electrotransfer properties of solution species. In this report, a new carbon-fiber working microelectrode was activated in the running buffer by applying +1.5 V for 15 min. By this method, the electrical resistance of the microelectrode was between 3 and 8 MΩ in 10 m*M* borate electrolyte.

Amperometric detection was performed using a two-electrode system. The microelectrode was fixed on an *xyz* micromanipulator of a microscope (Xicheng Optical Factory, Beijing, China), and was inserted into the detection capillary with the aid of another microscope. A Ag plate was used as a reference electrode. Potential control was provided and microcurrent detection was measured by a 901-μA analyser (Ningde Analytical Instrument Factory, Ningde, Fujian Province, China), and the current signal was recorded on a XWT recorder (Shanghai Dahua Instrument Factory, Shanghai, China).

2.5. Cyclic voltammetry

Cyclic voltammetry was performed on a 901-μA analyser with a two-electrode configuration, the same as the reference above, and with the electrochemical detection cell (d-H) as the electrochemical cell.

3. Results and discussion

3.1. Decoupler performance evaluation

For proper evaluation of the steady time and electric conductivity efficiency of a new decoupler, both similar CE systems apart from the one with the decoupler and the other without the decoupler of the separation capillary were used. Parameters were defined as follows: I_0=electrophoretic current without decoupler; I_i=initial electrophoretic current with a new decoupler while the high-voltage was applied immediately; I_s=steady electrophoretic current with a new decoupler; T_s=steady time when the electrophoretic current with a new decouple reached a stable value; $D_i=I_i/I_0$=initial electric conductivity efficiency; $D_s=I_s/I_0$=steady electric conductivity efficiency.

For an effective decoupler, the less T_s, the better; the larger D_i and D_s, the better. These parameters were tested for several decouplers. T_s, D_i and D_s (Table 1) were determined and calculated to be 16–20 min, 49–55% and 92–93%, respectively. Formal experiment can be started after the capillary with a new decoupler is equilibrated in the running buffer for at least 20 min.

A decrease in separation efficiency is not unexpected in a CE system that involves the use of a joint or fracture for electrochemical detection. For the proper evaluation of the effect of the decoupler on separation efficiency [theoretical number, $N=5.54(t_R/W_{0.5})^2$], two CE systems with the same separation conditions were used. The differences were that the 'reference' system employed UV detection without decoupler, meanwhile the system used on-column electrochemical detection with the decoupler.

Table 1
The steady time (T_s) and electric conductivity efficiency (D_i, D_0) of the decoupler[a]

Capillary dimension	Running time (min)	Electrophoretic current (μA)	T_s (min)	D_i (%)	D_s (%)
55.2 cm×50 μm[a]		20.8 (I_0)			
(55+2.0) cm[b]×50 μm	0	10.2 (I_i)	20	49.0	92.3
	2	10.5			
	4	11.2			
	6	12.3			
	8	13.7			
	10	15.2			
	12	16.9			
	14	17.5			
	16	18.3			
	18	18.8			
	20	19.2 (I_s)			
	22	19.3			
70.2 cm×75 μm		25.7 (I_0)			
(69+l.7) cm[c]×75 μm	0	14.2 (I_i)	16	55.2	93.4
	2	15.6			
	4	16.7			
	6	18.5			
	8	20.4			
	10	22.8			
	12	23.4			
	14	23.7			
	16	24.0 (I_s)			
	18	23.9			
	20	24.2			

[a] Working condition: running buffer, 10 m*M* Na_2HPO_4–10 m*M* NaH_2PO_4 (pH 6.8); applied voltage, 25 kV.
[b] Separation capillary length and detection capillary length with a decoupler.
[c] Separation capillary length and detection capillary length with a decoupler.

Table 2
Changes in theoretical plate number with and without the decoupler

Capillary dimension	Theoretical plate number (N)
55.2 cm×50 μm I.D.[a]	9.0×10^4
(55+2.0) cm×50 μm I.D.[b]	8.7×10^4
70.2 cm×75 μm I.D.[a]	2.3×10^4
(69.6+1.7) cm×75 μm I.D.[b]	2.2×10^4

[a] Working condition: running buffer, 10 m*M* Na_2HPO_4–10 m*M* NaH_2PO_4(pH 6.8); applied voltage, 25 kV; detection wavelength 280 nm; sample injection, 10 kV/5 s; test sample, *p*-diphenol (40 μg/ml).

[b] Working electrodes 100 μm length×10 μm O.D. (inserting) carbon fiber; detection potential, +1.0 V (vs. Ag); others, the same as note a.

Table 2 showed the changes in theoretical plate number with and without the decoupler. The theoretical plate number with the decoupler loses about 3.3% for a 50-μm I.D. capillary and 4.7% for a 75-μm I.D. capillary. These smaller changes of the theoretical plate number illustrated that there was no significant peak broadening, or interaction between the sample and ZD-61 glue of the decoupler

To evaluate the ability of the decoupler, fabricated by this method, to isolate the electrochemical detection from the high-voltage electric field or electrophoretic current, the detector noise i_b (background noise, pA) as a function of electrophoretic current I_e (μA) was determined and shown in Fig. 1. Fig. 1 showed that i_b increased dramatically with I_e above 11 μA without decoupler. Meanwhile the relationship between the applied voltages E(kV) and I_e was of linearity shown in Fig. 2. When the higher applied voltage was used, hydrogen gas was always produced at the carbon- fiber electrode with on-column detection. Background noise sharply increased and the bubbles formed in the capillary blocked the buffer flow. This phenomenon did not happen in end-column detection. However, by using the decoupler (5+2.0 cm, 50-μm diameter), the I_b from 3.5 to 4.9 pA increased slowly with the I_e from 10 to 65 μA (Fig. 3) under the conditions of 50 m*M* of borax running buffer. Similar trends were observed when the other running buffers were used, such as the Na_2HPO_4–NaH_2PO_4 system and etc. The noise level by using the borate system was higher than that by using the Na_2HPO_4–NaH_2PO_4 system. By using the later system, I_b values ranged from 0.9 to 1.5 pA. A similar noise level was obtained by the etched joint described in Ref. [12]. The results illustrated that the effect of the electrophoretic current on background noise was significantly suppressed due to the use of the decoupler.

The difference in results obtained with and without the decoupler by on-column amperometric CE–ED analysis of *o*-diphenol is shown in Fig. 4. The

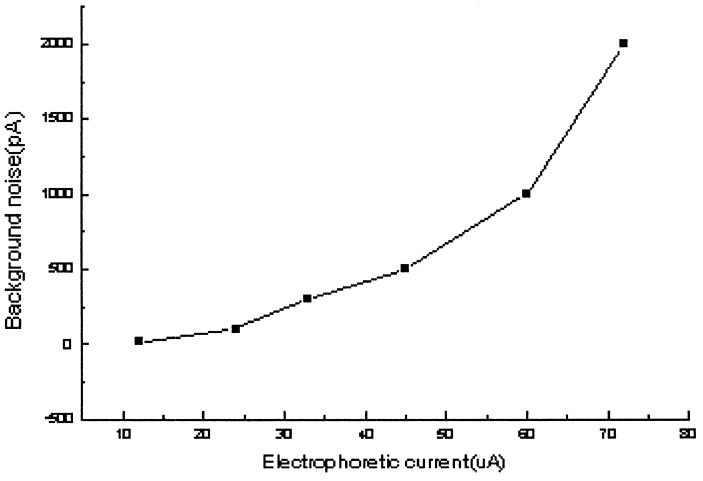

Fig. 1. Effect of the electrophoretic current on the background noise by CE–ED without decoupler. Capillary, 55.2 cm×50 μm I.D.; working electrode, 100 μm length×10 μm O.D. (inserting) carbon fiber; detection potential, +1.0 V (vs. Ag); running buffer: 50 mmol/l of borax.

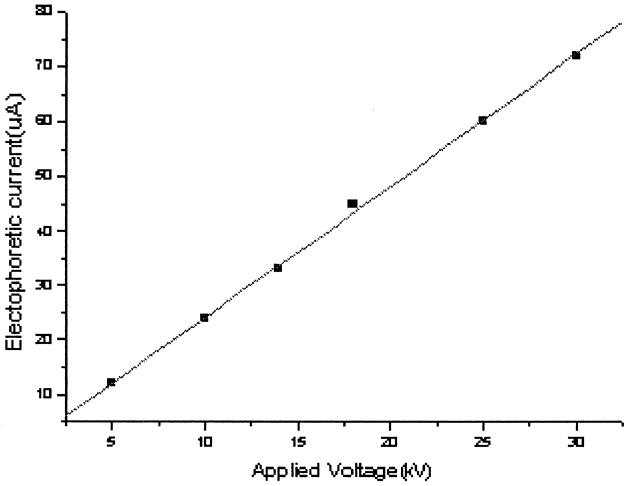

Fig. 2. Relationship between applied voltage and electrophoretic current by CE–ED without decoupler. Conditions as in Fig. 1.

peak height of *o*-diphenol with the decoupler was higher than that without the decoupler. This phenomenon resulted in a much more positive half-wave potential shift without the decoupler. Under the CE–ED with the decoupler, the half-wave potential was much closer to that observed in the bulk solution without the high applied voltage. This result coincides with that illustrated in Refs. [24–27].

3.2. Analysis of phenolic compounds by CE–ED with non-column amperometry with the decoupler

After electrochemical pretreatment, the carbon-fiber microelectrode (1 mm length×10 μm O.D.) was cycled in the background buffer of 10 m*M* Na_2HPO_4–NaH_2PO_4 (pH 6.5)–10 m*M* sodium dodecylsulfate (SDS)–5 m*M* β-cyclodextrin (β-CD)

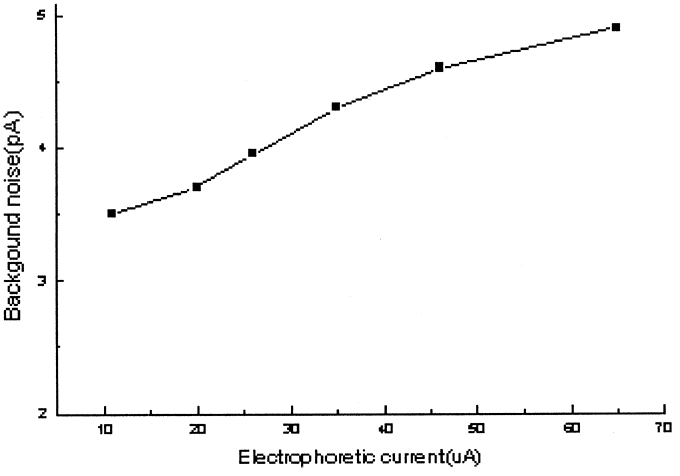

Fig. 3. Effect of electrophoretic current on the background noise by CE–ED with the decoupler. Capillary, (55+2.0) cm×50 μm I.D.; other conditions as in Fig. 1.

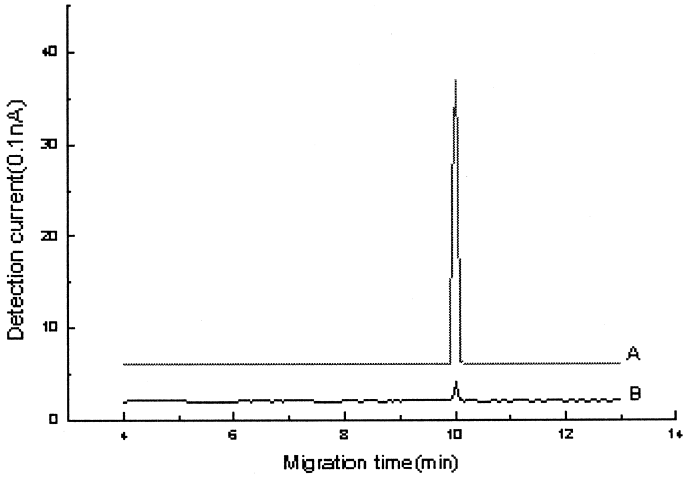

Fig. 4. Comparison between with (A) and without (B) the decoupler of CE–ED with on-column amperometry. Running buffer, 10 m*M* borax; capillary with the decoupler, (55+2.0) cm×50 μm I.D., other capillary without the decoupler 55.5 cm×50 μm I.D.; applied voltage, 15 kV; sample injection, 10 kV/5 s; working electrode, 150 μm length×10 μm O.D. (inserting) carbon fiber; detection potential, +0.95 V (vs. Ag); sample, *o*-diphenol (30 mg/l).

and in the samples of 10^{-4} mol/l of six *para*-substituted phenols, respectively. The whole irreversible anodic peak of *p*-nitrophenol was observed, the anodic current slowly increased above +1.1 V (vs. Ag). Irreversible anodic peaks for *p-tert.*-butylphenol at +0.85 V and *p*-bromophenol at +0.75 V, reversible anodic peaks for *p*-aminophenol at +0.31 V and for *p*-diphenol at +0.37 V, and whole reversible double anodic peaks for *p*-chlorophenol at +0.35 and +0.95 V were obtained. The anodic current for background solution was dramatically increased above +1.2 V.

Fig. 5 shows the the hydrodynamic voltammograms (HDVs) of four *para*-substituted phenols and buffer. Buffer [10 m*M* Na_2HPO_4–NaH_2PO_4 (pH 6.5)–10 m*M* SDS–5 m*M* β-CD] exhibited HDV in sharp increase from +1.2 V, while the four materials presented an increasing current HDV behavior from +0.95 V. As a compromise of high sensitivity and low background current, a +1.0 V value was selected for detection of six *para*-substituted phenols.

Fig. 6 shows the effect of the pH value on the migration time of these materials. With the pH value decreasing, the negative charges on the capillary inner wall are suppressed, and the migration time increases resulting from the electrophoretic mobilities of these materials. The SDS of the pseudo-stationary phase and the addition of β-CD enhanced the selectivity and resolutions in capillary electrokinetic chromatography, meanwhile SDS and β-CD influenced the redox potential and suppressed the detection current. As a compromise, 10 m*M* SDS and 5 m*M* β-CD were selected as the optimal concentration in the running buffer in CE–ED.

Under the optimal buffer, 10 m*M* Na_2HPO_4–NaH_2PO_4 (pH 6.5)–10 m*M* SDS–5 m*M* β-CD, electropherograms of six *para*-substituted phenols by CE–ED with on-column amperometric detection at the carbon-fiber microelectrode are shown in Fig. 7. The analytical data are listed in Tables 3 and 4. The detection limits were less than 0.40 mg/l except for *p*-nitrophenol and *p-tert.*-butylphenol. The recovery ranged from 96 to 106% (n=3). The results of the sample detection by this method were similar to those by high-performance liquid chromatography (LC-6A HPLC purchased from Shimadzu, Japan) with detection wavelength at 254 nm.

4. Conclusions

Fabrication of a decoupler isolating high-voltage

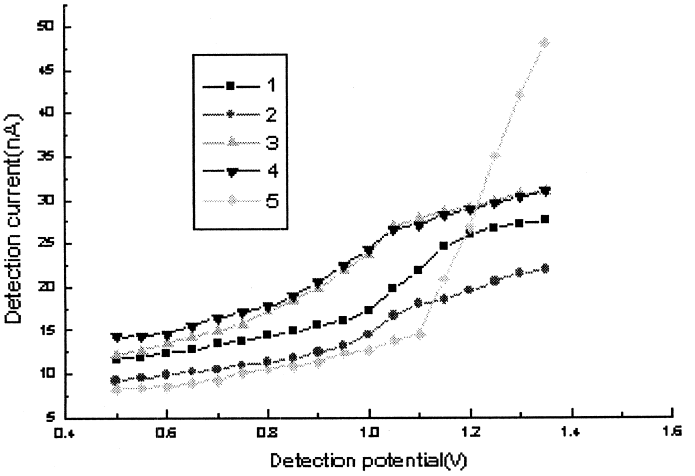

Fig. 5. Voltammetric behaviors of four *para*-substituted phenols and background buffer at the carbon-fiber microelectrode with the decoupler. Running buffer, 10 m*M* Na_2HPO_4–10 m*M* NaH_2PO_4–10 m*M* SDS-5 m*M* β-CD (pH 6.5); capillary with the decoupler, (64+1.7) cm×50 μm I.D.; applied voltage, 20 kV; sample injection, 10 kV/5 s; working electrode, 150 μm length×10 μm O.D. (inserting) carbon fiber; detection potential, from +0.50 V to +1.35 V (vs. Ag). Curves: 1, 20 mg/l *p*-diphenol; 2, 20 mg/l *p*-aminophenol; 3, 20 mg/l *p*-chlorophenol; 4, 200 mg/l *p*-nitrophenol; 5, 400-fold background noise.

electric field or electrophoretic current for on-column electrochemical detection with capillary electrophoresis by coupling laser focusing etching and HF etching provides a more durable joint with higher strength, shorter stable time, higher electric conductivity efficiency, lower noise level and less decrease of separation efficiency, together with an 85% success rate. The noise level by this decoupler was similar to that given by the reference [12]. The decoupler can be expected to be useful in the coupling of CE with conductivity detection, CE with potential detection, CE with inductively coupled plasma MS. Coupling with a carbon-fiber microelectrode (10 μm diameter) and practical small electrochemical detection cell, on-column amperometric detection of *para*-substituted phenols by ED with the

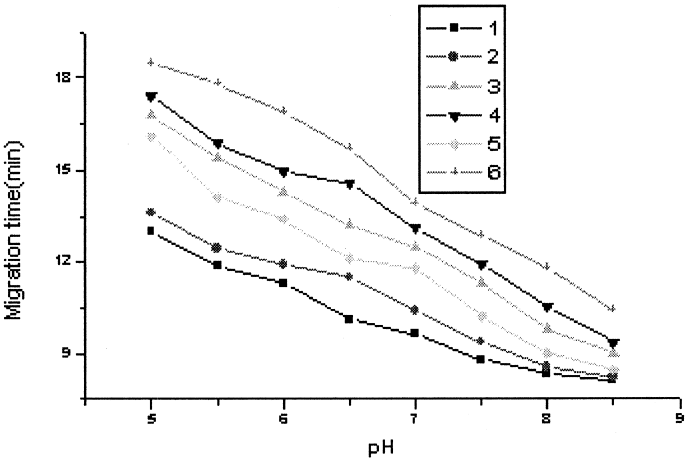

Fig. 6. Effect of the pH value on migration time of six *para*-substituted phenols. Detection potential, +1.0 V, pH value, from 8.5 to 5.0; other conditions as in Fig. 5. Curves: 1, *p*-aminophenol; 2, *p*-diphenol; 3, *p*-chlorophenol; 4, *p*-bromophenol; 5, *p*-nitrophenol; 6, *p-tert*.-butylphenol.

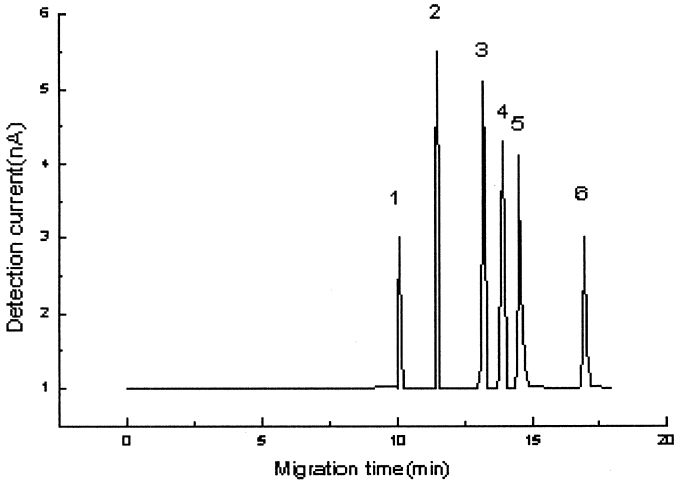

Fig. 7. Typical electropherogram of the six *para*-substituted phenols. Detection potential, +1.0 V (vs. Ag); other conditions as in Fig. 5. Peaks: 1, *p*-aminophenol (2 mg/l); 2, *p*-diphenol (5 mg/l); 3, *p*-chlorophenol (5 mg/l); 4, *p*-bromophenol (4 mg/l); 5, *p*-nitrophenol (30 mg/l); 6, *p-tert*.-butylphenol (20 mg/l).

Table 3
Calibration line and detection limits

Compound	Concentration range *C* (mg/l)	Calibration line ($I=a+bC$)		*r*	*n*	Detection limit (mg/l)
		a (pA)	*b* (pA·l/mg)			
p-Diphenol	0.5~50	6.3	990.2	0.9984	6	0.15
p-Aminophenol	0.5~50	9.2	951.4	0.9991	8	0.20
p-Chlorophenol	0.5~50	6.8	1012.5	0.9993	7	0.15
p-Nitrophenol	5.0~50	12.8	110.3	0.9986	6	2.50
p-Bromophenol	1.0~50	8.3	732.5	0.9976	7	0.40
p-tert.-Butylphenol	3.0~50	7.6	254.2	0.9975	6	2.20

Table 4
Results of the real sample[a]

Compound	Concentration of sample (mg/l)	Added concentration (mg/l)	Detected concentration (mg/l)	Recovery (%)	Detected concentration[b] (mg/l)
p-Diphenol	0.32±0.0 12	0.50	0.85±0.021	106.0	0.90±0.015
p-Aminophenol	ND[c]	1.50	1.45±0.024	96.7	1.50±0.020
p-Chlorophenol	ND[c]	1.50	1.53±0.019	102.0	1.51±0.025
p-Nitrophenol	3.42±0136	7.50	11.12±0.032	103.2	11.20±0.024
p-Bromophenol	ND[c]	5.00	4.85±0.038	97.0	4.70±0.030
p-tert.-Butylphenol	ND[c]	10.0	9.68±0.067	96.8	10.21±0.035

[a] The sample was obtained from the Qinyang Chemical Factory (Henan, China). After it was filtered through the 1.2-μm membrane, it was diluted with running buffer in 1:1 (v/v).

[b] The results were obtained by HPLC method with a C_{18}(250×4.6 mm I.D.) separation column, HAc–MeOH (5:95) as mobile phase, 1 ml/min as flow-rate, 254 nm as detection wavelength and 10 μl as injection volume.

[c] Not detected.

improved high-voltage electric field decoupler have been carried out.

Acknowledgements

The authors thank the Technology Tackle Foundation (TTF) of Henan Province (971120308), the Ninth Five-ear TTF of China (96-A23-01-06), the Natural Science Foundation (NSF) of China and NSF of Henan province for supporting this work.

References

[1] F.E.P. Mikkers, F.M. Everaerts, T.P.E.M. Verheggen, J. Chromatogr. 169 (1979) 11–20.
[2] J.W. Jorgenson, K.D. Lukacs, Anal. Chem. 53 (1981) 1298–1302.
[3] J.W. Jorgenson, K.D. Lukacs, J. Chromatogr. 218 (1981) 209–215.
[4] P. Gozel, E. Gassmann, H. Michelsen, R.N. Zare, Anal. Chem. 59 (1987) 44–49.
[5] S. Wu, N.J. Dovichi, J. Chromatogr. 480 (1989) 141–155.
[6] D. Chen, N.J. Dovichi, Anal. Chem. 68 (1996) 690–696.
[7] C.V. Owens, Y.Y. Davidson, S.A. Scoper, Anal. Chem. 69 (1997) 1256–1261.
[8] L. Reyderman, S. Stavchansky, Anal. Chem. 69 (1997) 3218–3222.
[9] R.A. Wallingford, A.G. Ewing, Anal. Chem. 59 (1987) 1762–1766.
[10] T.J. O'Shea, R.D. Greenhagen, S.M. Lunte, C.E. Lunte, M.R. Smyth, D.M. Radzik et al., J. Chromatogr. 593 (1992) 305–312.
[11] P.D. Voegel, W. Zhou, R.P. Baldwin, Anal. Chem. 69 (1997) 951–957.
[12] S. Hu, Z.L. Wang, P.B. Li, J.K. Cheng, Anal. Chem. 69 (1997) 264–267.
[13] J. Zhou, G.C. Gerhardt, A. Baranski, R. Cassidy, J. Chromatogr. A 839 (1999) 193–201.
[14] J. Zhou, D.M. Heckert, H. Zuo, C.E. Lunte, S.M. Lunte, Anal. Chim. Acta. 379 (1999) 307–317.
[15] Y.K. Yik, H.K. Lee, S.F.M. Li, S.B. Khoo, J. Chromatogr. 585 (1991) 139–144.
[16] I.C. Chen, C.W. Whang, J. Chromatogr. 644 (1993) 208–212.
[17] W.T. Kok, Y. Sahin, Anal. Chem. 65 (1993) 2497–2502.
[18] S. Park, S.M. Lunte, C.E. Lunte, Anal. Chem. 67 (1995) 911–918.
[19] S. Park, C.E. Lunte, Anal. Chem. 67 (1995) 4366–4370.
[20] X. Huang, R.N. Zare, Anal. Chem. 62 (1990) 443–446.
[21] I.C. Chen, C.W. Whang, J. Chin. Chem. Soc. (Taiwan) 41 (1994) 419–424.
[22] T. Kaneya, T. Imasaka, Anal. Chem. 67 (1995) 829–833.
[23] Z.B. Yuan, S.S. Zhang, H. Zou, Chinese J. Anal. Instrum. Newslett. 7 (1997) 198–201.
[24] F.M. Matysik, J. Chromatogr. 742 (1996) 229–234.
[25] G.C. Gerhardt, R.M. Cassidy, A.S. Baranski, Anal. Chem. 70 (1998) 2167–2173.
[26] F.M. Matysik, J. Chromatogr. A 802 (1998) 349–354.
[27] S.R. Wallenborg, L. Nyholm, C.E. Lunte, Anal. Chem. 71 (1999) 544–549.